Mater Renew Sustain Energy (2017) 6:5
DOI 10.1007/s40243-017-0089-1

ORIGINAL PAPER

Energy levels of natural sensitizers extracted from rengas (*Gluta* spp.) and mengkulang (*Heritiera elata*) wood for dye-sensitized solar cells

Nur ezyanie Safie[1] · Norasikin Ahmad ludin[1] · Norul Hisham Hamid[2] · Suhaila Sepeai[1] · Mohd Asri Mat Teridi[1] · Mohd Adib Ibrahim[1] · Kamaruzzaman Sopian[1] · Hironori Arakawa[3]

Received: 4 November 2016 / Accepted: 11 February 2017 / Published online: 18 February 2017

Abstract Dye-sensitized solar cells (DSSCs) are fabricated using natural sensitizers extracted from rengas (*Gluta* spp.) and mengkulang (*Heritieraelata*) wood. The natural sensitizers are extracted using a cold extraction and the Soxhlet extraction methods. This paper presents the results of the analysis of the optical characteristics of the sensitizers via ultraviolet–visible spectrophotometry and Fourier transform infrared spectroscopy. The optical band gap and the highest occupied molecular orbital (HOMO)–lowest unoccupied molecular orbital (LUMO) levels of each investigated sensitizer are calculated on the basis of the analyzed data collected from photoluminescence and cyclic voltammetry. The DSSCs with the mengkulang sensitizer have better conversion efficiency ($\eta = 0.1695\%$) than the DSSCs with the rengas sensitizer ($\eta = 0.109\%$). The performance of the DSSCs indicates an increment as the ratios of the mixed mengkulang:rengas (60%:40%) and mengkulang:rengas (40%:60%) sensitizers increase up to 0.296 and 0.292%, respectively.

Keywords Optical band gap · HOMO–LUMO level · Natural sensitizer · DSSCs

✉ Norasikin Ahmad ludin
sheekeen@ukm.edu.my

[1] Solar Energy Research Institute (SERI), Universiti Kebangsaan Malaysia, 43600 Bangi, Selangor, Malaysia

[2] Faculty of Forestry, Universiti Putra Malaysia, 43400 Serdang, Selangor, Malaysia

[3] Department of Industrial Chemistry, Faculty of Engineering, Tokyo University of Science, Tokyo 162-0826, Japan

Introduction

In the critical view of renewable energy forms, solar energy has shown its potentials for power generation market especially in the Malaysia region that have constant supply of sun radiation throughout the year. Dye-sensitized solar cells (DSSCs) as the third generation solar cells devices have attract a lot of attention from researches as it is low cost and have potential for high photoconversion efficiency as reported by Gratzel group which have obtained efficiency up to 12% [1–4]. The components that build up the mechanism in DSSC including porous semiconductor loaded with sensitizer on a glass substrate, redox couple electrolyte, and counter electrode [5]. Sensitizer becomes one of the important components that attract research interest to enhance the device performance. From the metal complex to metal free sensitizer and from inorganic to organic type of sensitizers, they have their own potentials and drawbacks. However, metal complex such as Ruthenium and Zinc porphyrin dye have been reported to achieve better performance which are 12–13% efficiency as compared to others [6–10]. However, the costing and synthesis issues have leads to intense interest to use other than metal complex sensitizers even though the performance of other type of sensitizer are still considered low [11].

The performance of DSSCs depends on sensitizers that act as light harvesters in the mechanism. The best sensitizers must be capable of absorbing a wide range of visible light and producing electrons [12]. Natural dyes provide different types of pigments and thus serve as alternative sensitizers for inexpensive organic-based DSSCs. The requirements that natural dyes should meet are as follows:(1) ability to absorb a wide range of visible and near-infrared photons, (2) presence of an anchoring group that

can strongly attach to the mesoporous oxide layer, and (3) an energy level that is between the lowest unoccupied molecular orbital (LUMO) and the highest occupied molecular orbital (HOMO) for an efficient electron injection from the valence to the conduction bands of the semiconductors [13]. Superior sensitizers should also be able to absorb all of the light that strikes below a threshold wavelength (920 nm) and convert standard air mass (AM) of 1.5 sunlight into electricity, so that upon excitation, these sensitizers could inject electrons from the dyes into the solid materials with a quantum yield of unity [14]. In considering natural dyes as one of the parameters in the development of DSSCs, verifying the efficiency with respect to processes such as (1) the absorption of incident photons by the dye molecules, (2) conversion of photons to electron–hole pairs, and (3) separation and collection, before choosing pigments as sensitizers is important [15].

The interest in this study is towards effective natural sensitizers. In the last two decades, a number of studies have tested variable plant parts, such as flowers, leaves, barks, and roots, in search of effective natural sensitizers. However, most of the studies in the open literature did not investigate potential sensitizers extracted from the wood of forest trees. Malaysia is known for the biodiversity of its tropical rainforests that are home to various tree species. Hence, exploring the contribution of trees to fields other than the furniture industry, such as the field of solar energy, is important. The present study introduces sensitizers extracted from rengas (*Gluta* spp.) and mengkulang (*Heritieraelata*) wood and examines their optical properties and performance in DSSCs. In addition, the ratios of the mixtures of these sensitizers are manipulated to investigate their effectiveness on device performance.

Methodology

Materials

Rengas and mengkulang wood were collected from a local sawmill in Kuala Lumpur, Malaysia, TiO_2 paste (WER 2, Dyesol), fluorine-doped conducting tin oxide (FTO) glasses ($\sim 15\ \Omega\ sq^{-1}$, Solaronix), redox electrolyte (iodolyte AN-50, Solaronix), platinum paste purchased from Solaronix, Surlyn (60 μm, Maltonix), organic solvent purchased from Sigma-Aldrich.

Wood extraction

A wood chipper machine and a knife ring chipper were used to obtain fine particles from the wood. The particles were then dried in an oven at 60 °C for 24 h before undergoing a screening process to isolate the particle size. The large particles must be fined using a ball mill. The sawdust obtained was then dried in an oven at 130 °C for 24 h to reduce its moisture content. To extract dye from the sawdust, methanol was used as the organic solvent in the cold extraction technique. The sawdust was soaked in methanol (1:10 w/v ratio) and left overnight at room temperature. All of the extraction procedures were implemented under dim conditions, and the glassware containing the dyes were covered with aluminum foil to minimize photooxidation. Subsequently, the mixture was subjected to the Soxhlet extraction technique to obtain the extractive compound. The crude extract was stored in refrigerator (4 °C) for future use. In addition to the individual sensitizers, mixtures of both sensitizers were prepared with three different v/v ratios and were classified as mengkulang:rengas (60%:40%), mengkulang:rengas (40%:60%), and mengkulang:rengas (50%:50%).

Fabrication of dye-sensitized solar cells

Photo electrodes were prepared by depositing TiO_2 paste (WER 2, Dyesol) into fluorine-doped conducting tin oxide (FTO) glasses ($\sim 15\ \Omega\ sq^{-1}$, Solaronix), which were used as the conductive glass plates in the doctor blading technique. The electrodes were then sintered at 450 °C for 30 min. The photo electrodes were subsequently dipped in the sensitizers, that is, mengkulang (M), rengas (R), and their mixtures [M:R (50%:50%), M:R (60%:40%), and M:R (40%:60%)] for 24 h at room temperature to allow sufficient time to graft the dye molecules on the TiO_2 surface. Then, TiO_2 electrodes were extracted and rinsed with methanol before being dried with nitrogen gas. The DSSCs were assembled by introducing a redox electrolyte (iodolyte AN-50, Solaronix) between the dyed TiO_2 electrode and the platinum counter electrode. The platinum paste purchased from Solaronix was deposited on to the FTO glasses ($\sim 8\ \Omega\ sq^{-1}$, Solaronix) and heated at 450 °C for 30 min. Surlyn (60 μm, Maltonix) was used to assemble the photo and counter electrodes of the cells.

Characterization and device performance

The absorption spectra were analyzed via ultraviolet–visible (UV–Vis) absorption spectroscopy (Shimadzu UV-1800). The functional groups of the sensitizers were determined via Fourier transform infrared spectroscopy (FTIR) (Perkin Elmer Spectrum 400 FT-IR). The HOMO and LUMO levels were determined via photoluminescence (PL) (FLSP920 Edinburgh Instrument) and cyclic voltammetry (CV) (ModuLab Solartron Analytical).

The current–voltage (*I–V*) measurement was conducted using solar simulator class AAA (XES-40S1, San-Ei Electrical) under irradiation of 1000 W/m^2. The maximum

power conversion efficiency (ŋ) was calculated using the following formula:

$$\eta = ff \times I_{sc} \times V_{oc}/P,$$

where ff is the fill factor, I_{sc} is the short circuit photo current density (A/cm^2), V_{oc} is the open circuit voltage (V), and P is the intensity of the incident light (W/cm^2) of the DSSC.

The fill factor was defined using the following relation:

$$FF = (I_{\max} \times V_{\max})(I_{sc} \times V_{oc}),$$

where I_{max} and V_{max} represent the maximum output values of the current and voltage, respectively; and I_{sc} and V_{oc} represent the short circuit current and open circuit voltage, respectively. The incident photon-to-current efficiency (IPCE) was also measured via spectral response measurement (IVT Solar PVE-300, Bentham).

Result and discussion

UV–Vis absorption spectra

The extracted crude sensitizers from rengas and mengkulang wood were examined under a UV–Vis spectrophotometer with methanol as the reference solvent. The absorption spectra for the crude sensitizers are presented in Fig. 1. The intense peak was observed between 400 and 512 nm for the rengas sensitizer. However, a broad shoulder representing the mengkulang sensitizer appeared between 420 and 550 nm. Therefore, the rengas sensitizer demonstrated strong absorption at a low wavelength. Figure 2 illustrates the absorption spectra of the mixtures of the mengkulang and rengas sensitizers with three different percentage ratios. The absorption spectra of all the mixed sensitizers were similar to those of the rengas sensitizer because the chemical characteristic of this sensitizer was more dominantly absorbed onto the TiO_2 surface compared with that of the mengkulang sensitizer. The absorption spectra of the mixed sensitizers absorbed onto the TiO_2 surface are illustrated in Fig. 2. The spectra after the grafting process did not show an obvious peak, but a wide shoulder was observed between 400 and 600 nm. The UV–Vis absorption of TiO_2 without a sensitizer is also presented in this work for comparison. The absorption spectra of the sensitizers grafted on TiO_2 showed a stable and broad shoulder, enabling the harvest of light in a broad spectrum of solar energy, ultimately leading to the production of high photocurrent in DSSC device [16].

The main dye of rengas sensitizer identified was anthocyanin based on the intense peak observed between 400 and 512 nm [17]. Anthocyanins are the largest group of water-soluble pigments widespread in the plant kingdom. The anthocyanins belong to the group of natural dyes responsible for several colors in the red–blue range, found in fruits, flowers and leafs of plants. Carbonyl and hydroxyl groups present in the anthocyanin molecule can be bound to the surface of a porous TiO_2 film (Fig. 3). This makes electron transfer from the anthocyanin molecule to the conduction band of TiO_2.

FTIR analysis

The analysis of the functional groups of the sensitizers was conducted using FTIR spectroscopy, with KBr as the reference background. Figure 4 shows that the IR spectra patterns of all the samples were similar because the functional groups present in the samples were the same. The broad band observed at 3323, 3309, 3324, and 3319 cm^{-1} was due to the presence of vibrations of the free hydroxyl group (Ar–O-H) of phenols. The small and intense peaks at

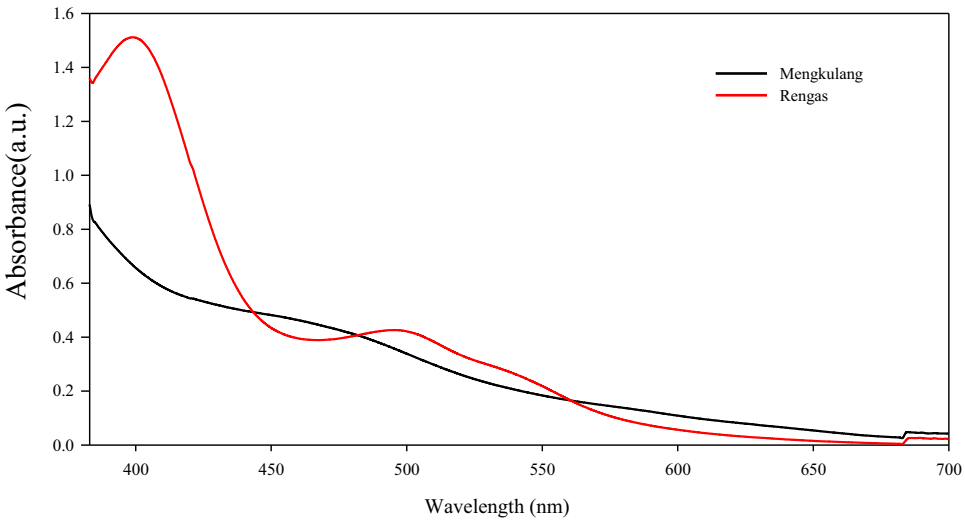

Fig. 1 UV–Vis absorption spectra of mengkulang and rengas sensitizers

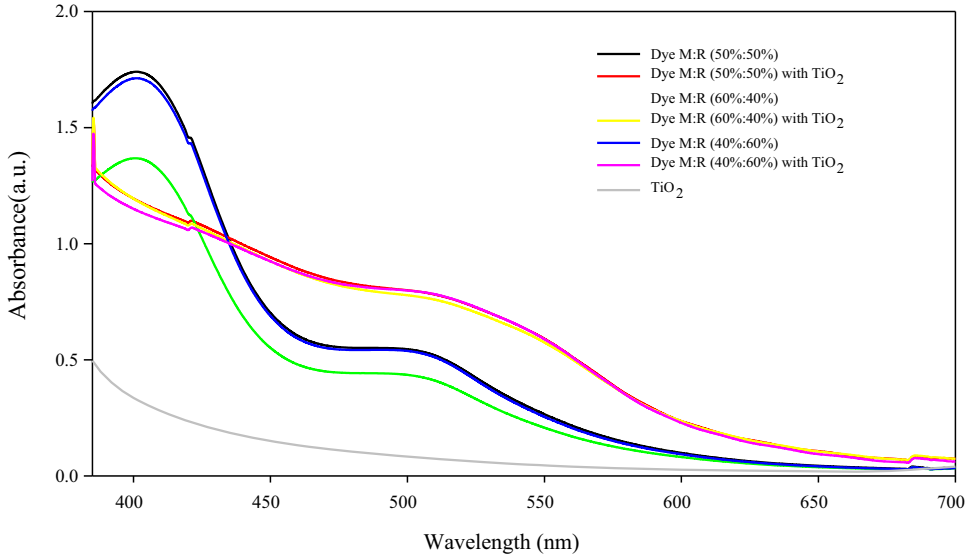

Fig. 2 UV–Vis absorption of mixed dyes, TiO_2 electrode, and dyes adsorbed onto TiO_2 (M:R is mengkulang:rengas)

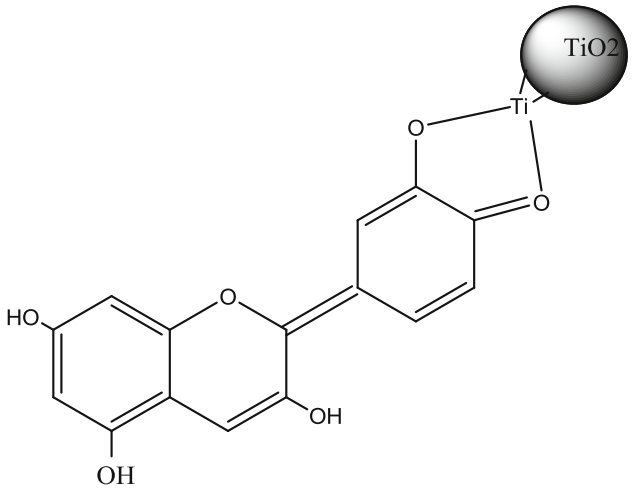

Fig. 3 The chemical structure of anthocyanin

2832 and 2944 cm^{-1} were attributed to the sp^3 C–H bond stretching. The small shoulder that appeared at 1449 cm^{-1} was attributed to the aromatic C=C stretching. All of the mixed sensitizers comprised similar functional groups, such as hydroxyl group, C–H bond, and aromatic C=C.

Optical band gap and HOMO–LUMO calculations

The optical band gap was measured using PL while the HOMO–LUMO levels were calculated using CV analysis [9]. The optical band gap of the sensitizers was obtained from the relation $E_g^{opt} = hc/\lambda$, where h is Planck's constant, c is the speed of light, and λ is the emission peak obtained from the PL emission spectra. Table 1 provides the optical band gap measurement of all the samples in this study. Compared with the rengas sensitizer, the mengkulang

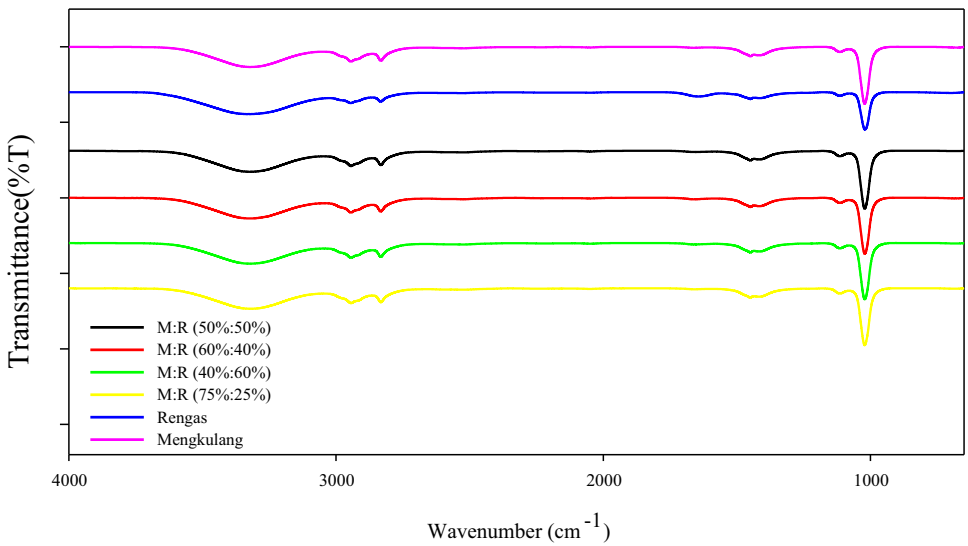

Fig. 4 FTIR analysis of individual and mixed sensitizers

Table 1 Summary of optical band gap measurement

Sensitizer	λ max (nm)	$E_g^{opt} = hc/\lambda$ (eV)
Mengkulang	522	2.38
Rengas	576	2.15
M:R (50%:50%)	569	2.18
M:R (40%:60%)	573	2.16
M:R (60%:40%)	572	2.17

sensitizer showed a higher optical band gap value of 2.38 eV from the emission peak of 522 nm. However, the other samples indicated a close band gap value between 2.15 and 2.18 eV. The emission peaks obtained for the M:R (50%:50%), M:R (60%:40%), and M:R (40%:60%) mixtures were 569, 572, and 573 nm, respectively. As shown in Fig. 5, only the mengkulang sensitizer exhibited a broad emission peak, whereas the other sensitizers displayed similar emission peak patterns.

The cyclic voltammograms of the mengkulang, rengas, and mixed sensitizers are presented in Fig. 6. The cyclic voltammetry measurements involved three electrodes, namely, glassy carbon working electrode, platinum counter electrode, and Ag/AgCl reference electrode, at a scan rate of 100 mV/s. The calculated positions of the HOMO and LUMO levels are provided in Table 2. HOMO level (E_{HOMO}) was determined with respect to their respective oxidation potential onset as extrapolated from the voltammograms of the sensitizers [18] using the equation

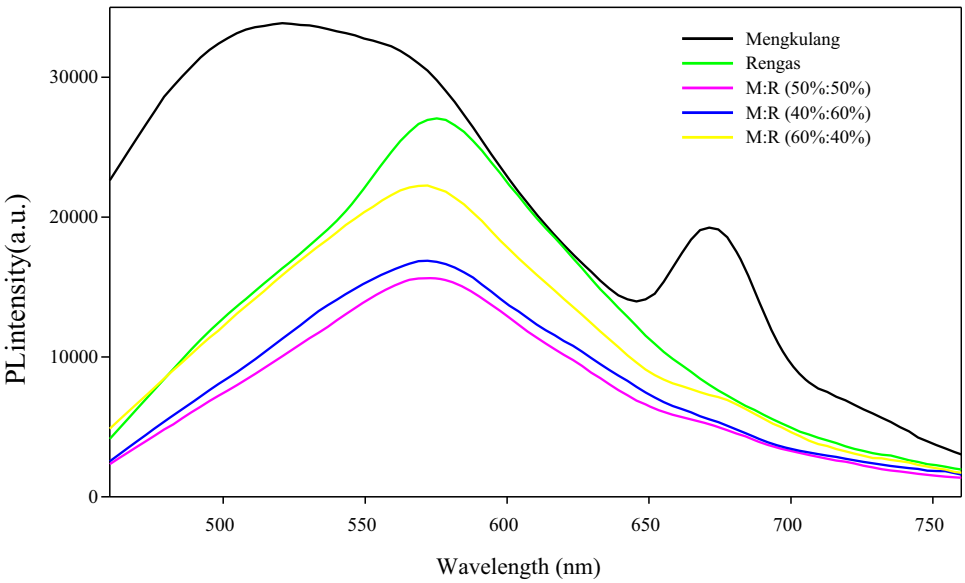

Fig. 5 Emission spectra of individual and mixed sensitizers

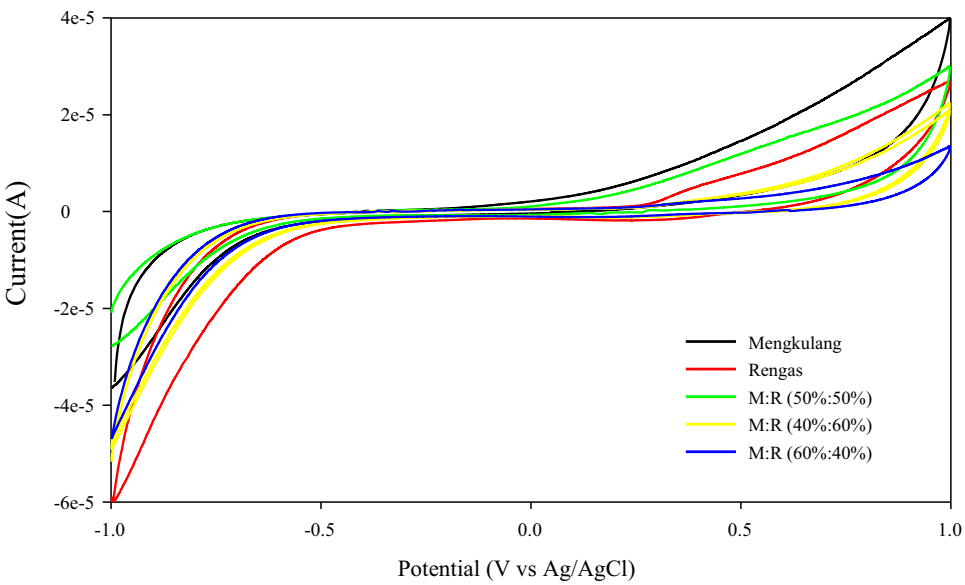

Fig. 6 Cyclic voltammograms of individual and mixed sensitizers (M:R is Mengkulang:Rengas)

Table 2 Calculated HOMO–LUMO energy levels and optical band gap measurement

Sensitizer	E_g^{opt}(eV)	E_{ox}^{onset} vs Ag/AgCl (V)	E_{LUMO} (eV)	E_{HOMO} (eV)
Mengkulang	2.38	0.29	−2.31	−4.69
Rengas	2.15	0.26	−2.51	−4.66
M:R (50%:50%)	2.18	0.21	−2.43	−4.61
M:R (40%:60%)	2.16	0.32	−2.56	−4.72
M:R (60%:40%)	2.17	0.22	−2.45	−4.62

$E_{HOMO} = -(4.4 + E_{ox}^{onset}))$ (eV). This indicates that the energy levels obtained have a difference of 4.4 eV from the vacuum level. The LUMO level is the addition of HOMO level and optical band gap of sensitizers, $E_{LUMO} = E_{HOMO} + E_g^{opt}$ [19–21]. Exactly 0.1 M of lithium perchlorate ($LiClO_4$) was used as the supporting electrolyte. On the basis of the HOMO–LUMO levels presented in Table 2, Fig. 7 presents a schematic diagram for comparing the energy levels of the investigated sensitizers in terms of vacuum level and normal hydrogen electrode (NHE).

The conduction band (CB) of TiO_2 was reported to locate around −4 to −4.3 eV [22, 23]. In this study, LUMO levels of the individual sensitizers and mixed sensitizers were located more positive from CB of TiO_2 with respect to the vacuum level (Fig. 7). The LUMO levels of sensitizers must be located slightly above the energy levels of semiconductors so that sensitizers can inject electrons into the conduction band of TiO_2 with high quantum yields [24]. Ooyama and Harima [25] reported that the desire difference of LUMO level of sensitizer and CB of TiO_2 should be more than 0.2 eV. Even though the LUMO levels of all investigated sensitizers were found to be more than 0.2 eV, this condition should be followed with efficient dye regeneration by electron transfer from the redox couple in the electrolyte to obtain high efficiency device. The HOMO level of sensitizer must be more negative than the redox potential with respect to the vacuum level in the range of 0.2–0.3 eV [26]. From the previous study, the redox potential of I_3^-/I^- redox couple was reported to locate in the range of −4.6 to −5 eV [4, 5, 27, 28]. However, HOMO level calculated in this study is located in the range of redox potential. This may contribute to the poor dye regeneration and hence lead to the poor performance of these devices.

Current–voltage (I–V) characteristics

Figure 8 illustrates the *I–V* curve of the individual mengkulang and rengas sensitizers and their mixtures. The performances of the DSSCs are calculated and tabulated in Table 3. The best performance was exhibited by the mixed sensitizer M:R (60%:40%), which achieved a conversion efficiency (ŋ) of 0.295% given an open circuit voltage (V_{oc}) of 0.528 V, a short circuit current density (J_{sc}) of 0.9 mA/cm^2, and a fill factor (*ff*) of 62.16 under the irradiance of 1000 W/m^2. The mixed sensitizer M:R (40%:60%) indicated slightly similar results, with its conversion efficiency (ŋ) calculated at 0.292% given an open circuit voltage (V_{oc}) of 0.526 V, a short circuit current density (J_{sc}) of 0.9 mA/cm^2, and a fill factor (*ff*) of 61.78. Furthermore, the mixed sensitizer M:R (50%:50%) showed a conversion efficiency (ŋ) of 0.205% given an open circuit voltage (V_{oc}) of 0.540 V, a short circuit current density (J_{sc}) of 0.6 mA/

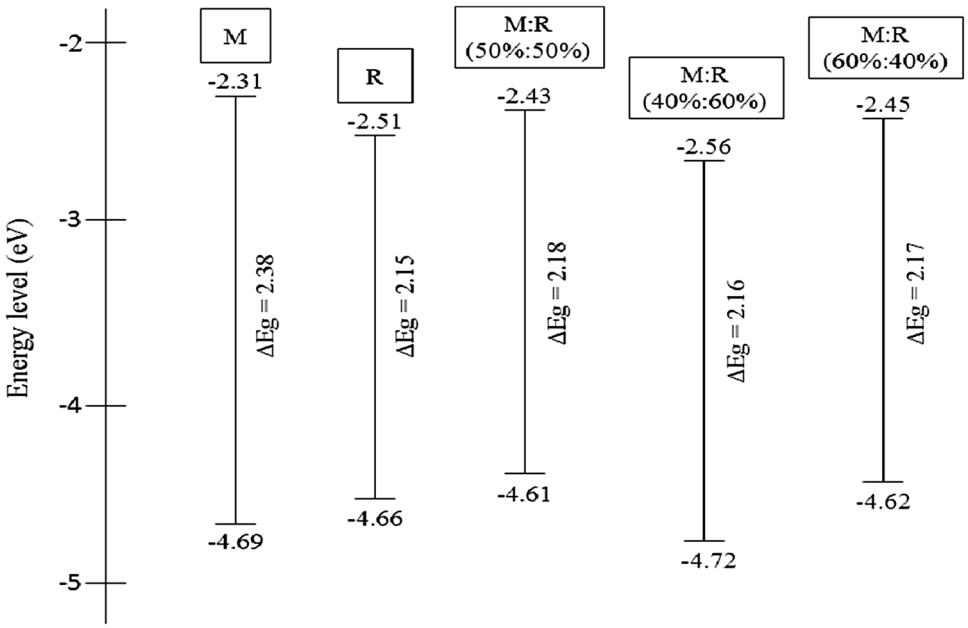

Fig. 7 Schematic diagram of the comparison of the energy level of the investigated sensitizers in terms of vacuum level and NHE (*M* stands for mengkulang, *R* indicates rengas)

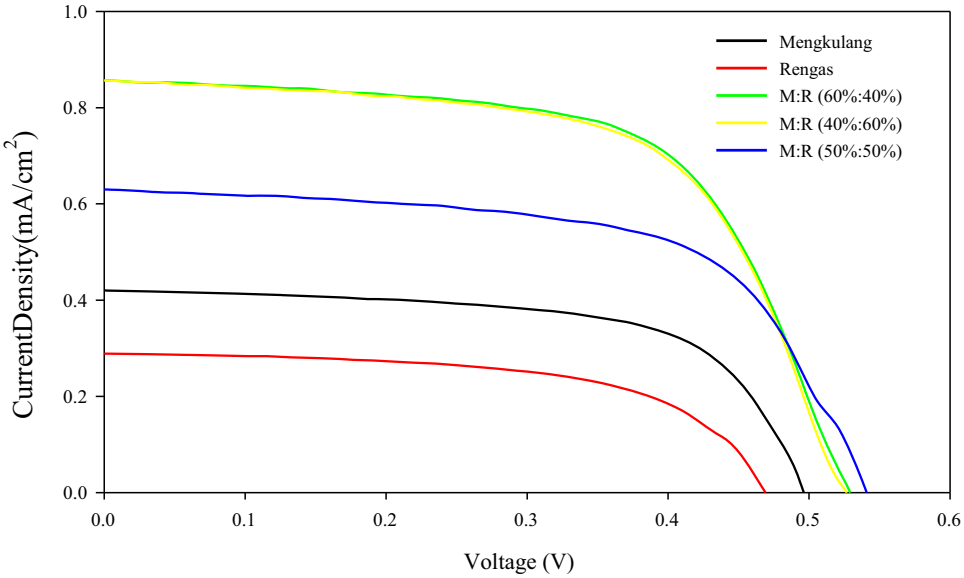

Fig. 8 Comparison of *I–V* characteristics of individual and mixed sensitizers

Table 3 Current–voltage (*I–V*) characteristics and power conversion efficiencies (ŋ) of DSSCs sensitized with different type of sensitizers

Sensitizer	V_{oc} (V)	J_{sc} (mA cm^{-2})	*ff*	*η*/ %
Mengkulang	0.53	0.40	75.98	0.16
Rengas	0.50	0.30	72.88	0.11
M:R (50%:50%)	0.54	0.60	63.28	0.21
M:R (40%:60%)	0.53	0.90	61.78	0.29
M:R (60%:40%)	0.53	0.90	62.16	0.30

cm^2, and a fill factor (*ff*) of 63.28. Overall, as an individual sensitizer the mengkulang sensitizer achieved higher conversion efficiency (ŋ) of 0.161% given an open circuit voltage (V_{oc}) of 0.529 V, a short circuit current density (J_{sc}) of 0.4 mA/cm^2, and a fill factor (*ff*) of 75.98. Whereas the rengas sensitizer achieved conversion efficiency (ŋ) of 0.109% given an open circuit voltage (V_{oc}) of 0.5 V, a short circuit current density (J_{sc}) of 0.3 mA/cm^2, and a fill factor (*ff*) of 72.88.

The energy conversion efficiency (ŋ) of the mixed sensitizers was higher because of the value of J_{sc} is higher than that of the individual sensitizers. The value of J_{sc} indicates strong interaction of TiO_2 with sensitizer in photoanode and their capability to absorb light that lead to high electron-injection efficiency [25, 29, 30].

IPCE spectra

Figure 9 shows the IPCE spectra of all of the investigated sensitizers. The mixed sensitizers M:R (60%:40%) and

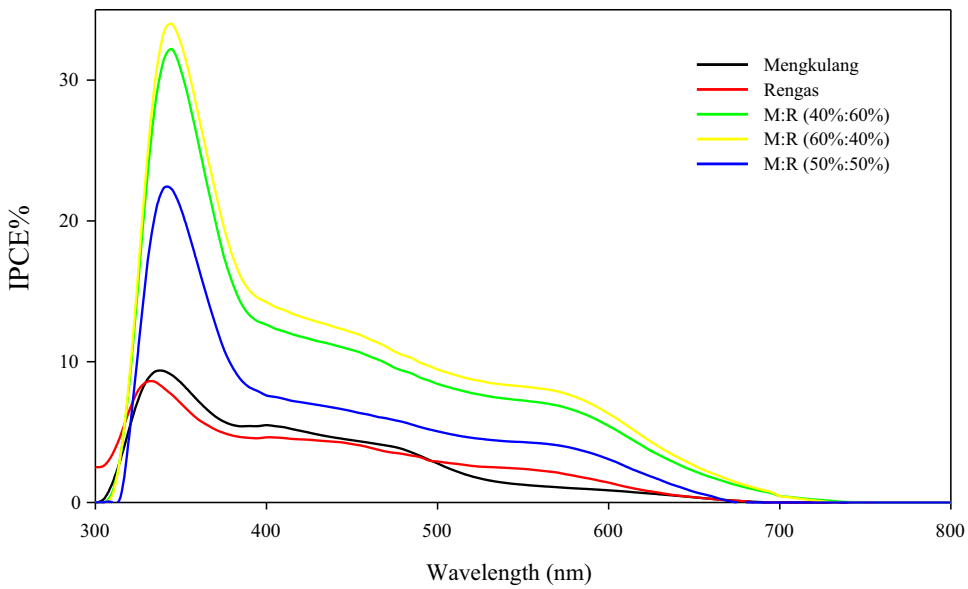

Fig. 9 IPCE spectra of individual and mixed sensitizers

M:R (40%:60%) showed as light increment in the IPCE percentage, followed by the mixed sensitizer M:R (50%:50%). The individual sensitizers achieved a lower IPCE percentage than the mixed sensitizers. This result is parallel to the low efficiencies of the individual sensitizers based on their *I–V* characteristics. The IPCE percentages obtained agree with the *I–V* data collected in this study as well as with the findings of Kumara et al. [18], who found that the low efficiency of IPCE contributes to the low energy conversion efficiency (ŋ) of DSSCs. In addition, the current produce might be low because electrons are not being able to move smoothly through semiconductor and contribute to recombination. This effect of recombination in DSSCs also leads to low percentage of IPCE.

Conclusion

In summary, the current study reveals potential of natural sensitizers extracted from rengas and mengkulang wood. The best performance was obtained when the sensitizers were mixed at a ratio of 60%:40% (M:R). The HOMO and LUMO levels of all of the investigated sensitizers were calculated. The optical band gap value decreased when the sensitizers were mixed. The individual rengas and mengkulang sensitizers exhibited lower energy conversion efficiencies (ŋ) than their mixed forms. The low IPCE percentage was found to contribute to the low energy conversion efficiencies (ŋ) of the DSSCs, with the individual sensitizers achieving a lower IPCE than their mixed forms. The efficiencies obtained using these sensitizers remain low for large-scale practical applications, but the results may serve as a reference for future studies on these new natural sensitizers.

Acknowledgement This research was supported by Universiti Kebangsaan Malaysia and Ministry of Higher Education Malaysia (MOHE) under Iconic Collaboration Grant (ICONIC-2013-006) and Look East Policy Grant (LEP 2.0/14/UKM/NT/03/1).

References

1. Chen, C., Wang, M., Li, J., Pootrakulchote, N., Alibabaei, L., Decoppet, J., Gra, M.: Highly efficient light-harvesting. ACS Nano **3**(10), 3103–3109 (2009)
2. Liu, B., Li, W., Wang, B., Li, X., Liu, Q., Naruta, Y., Zhu, W.: Influence of different anchoring groups in indoline dyes for dye-sensitized solar cells: electron injection, impedance and charge recombination. J. Power Sour. **234**, 139–146 (2013)
3. Liang, M., Chen, J.: Arylamine organic dyes for dye-sensitized solar cells. Chem. Soc. Rev. **42**, 3453–3488 (2013)
4. Zang, X., Huang, Z., Wu, H., Iqbal, Z., Wang, L., Meier, H., Cao, D.: Molecular design of the diketopyrrolopyrrole-based dyes with varied donor units for efficient dye-sensitized solar cells. J. Power Sour. **271**, 455–464 (2014)
5. Dou, Y., Wu, F., Fang, L., Liu, G., Mao, C., Wan, K.: Enhanced performance of dye-sensitized solar cell using Bi 2 Te 3 nanotube/ZnO nanoparticle composite photoanode by the synergistic effect of photovoltaic and thermoelectric conversion. J. Power Sour. **307**, 181–189 (2016)
6. Yella, A., Lee, H.W., Tsao, H.N., Yi, C., Chandiran, A.K., Nazeeruddin, M.K., Gratzel, M.: Porphyrin-sensitized solar cells with cobalt (II/III)-based redox electrolyte exceed 12 percent efficiency. Science **334**(6056), 629–634 (2011)
7. Hagfeldt, A., Boschloo, G., Sun, L., Kloo, L., Pettersson, H.: Dye-sensitized solar cells. Chem. Rev. **110**, 6595–6663 (2010)
8. Cao, Y., Bai, Y., Yu, Q., Cheng, Y., Liu, S., Shi, D., Wang, P.: Dye-sensitized solar cells with a high absorptivity ruthenium sensitizer featuring a 2- (Hexylthio) thiophene conjugated bipyridine. Alcohol **113**, 6290–6297 (2009)
9. Leonat, L., Sbârcea, G., Brañzoi, I.: Cyclic voltammetry for energy levels estimation of organic materials. Sci. Bull. Ser. **75**, 111–118 (2013)
10. Mathew, S., Yella, A., Gao, P., Humphry-Baker, R., Curchod, B.F.E., Ashari-Astani, N., Grätzel, M.: Dye-sensitized solar cells with 13% efficiency achieved through the molecular engineering of porphyrin sensitizers. Nat. Chem. **6**(3), 242–247 (2014)
11. Calogero, G., Bartolotta, A., Di Marco, G., Di Carlob, A., Bonaccorso, F.: Vegetable-based dye-sensitized solar cells. Chem. Soc. Rev. (2015). doi:10.1039/c4cs00309h
12. Smestad, G.P.: Demonstrating electron transfer and nanotechnology: a natural dye—sensitized nanocrystalline energy converter. J. Chem. Educ. **75**(6), 752–756 (1998)
13. Gong, J., Liang, J., Sumathy, K.: Review on dye-sensitized solar cells (DSSCs): fundamental concepts and novel materials. Renew. Sustain. Energy Rev. **16**(8), 5848–5860 (2012)
14. Grätzel, M.: Conversion of sunlight to electric power by nanocrystalline dye-sensitized solar cells. J. Photochem. Photobiol. **164**(1–3), 3–14 (2004)
15. Narayan, M.R.: Review: dye sensitized solar cells based on natural photosensitizers. Renew. Sustain. Energy Rev. **16**(2012), 208–215 (2011)
16. Lim, A., Manaf, N.H., Tennakoon, K., Chandrakanthi, R.L.N., Biaw, L., Lim, L., Ekanayake, P.: Higher performance of DSSC with dyes from *Cladophora* sp. as mixed cosensitizer through synergistic effect. J. Biophys. **2015**, 8 (2015)
17. Mounir, A., Ahmad, S.A., Wael Doubal, A.: Studying of natural dyes properties as photo-sensitizer for dye-sensitized solar cells. J. Electron. Dev. **16**, 1370–1383 (2012)
18. Kumara, N.T.R.N., Ekanayake, P., Lim, A., Iskandar, M., Ming, L.C.: Study of the enhancement of cell performance of dye sensitized solar cells sensitized with *Nephelium lappaceum* (F: Sapindaceae). J. Solar Energy Eng. **135**(August), 031014 (2013)
19. Cardona, C.M., Li, W., Kaifer, A.E., Stockdale, D., Bazan, G.C.: Electrochemical considerations for determining absolute frontier orbital energy levels of conjugated polymers for solar cell applications. Adv. Mater. **23**(20), 2367–2371 (2011)
20. Zhou, J., Xie, S., Amond, E.F., Becker, M.L.: Tuning energy levels of low bandgap semi-random two acceptor copolymers. Macromolecules **46**(9), 3391–3394 (2013)

21. Ledwon, P., Brzeczek, A., Pluczyk, S., Jarosz, T., Kuznik, W., Walczak, K., Lapkowski, M.: Synthesis and electrochemical properties of novel, donor-acceptor pyrrole derivatives with 1,8-naphthalimide units and their polymers. Electrochim. Acta **128**, 420–429 (2014)
22. Nazeeruddin, M.K., Péchy, P., Renouard, T., Zakeeruddin, S.M., Humphry-Baker, R., Cointe, P., Grätzel, M.: Engineering of efficient panchromatic sensitizers for nanocrystalline TiO2-based solar cells. J. Am. Chem. Soc. **123**, 1613–1624 (2001)
23. Lim, A., Kumara, N.T.R.N., Ling, A., Huq, A., Chandrakanthi, R.L.N., Iskandar, M., Ekanayake, P.: Potential natural sensitizers extracted from the skin of Canarium odontophyllum fruits for dye-sensitized solar cells. Spectrochimica. Acta. Part. A. **138**, 596–602 (2015)
24. Kumara, N.T.R.N., Ekanayake, P., Lim, A., Liew, L.Y.C., Iskandar, M., Ming, L.C., Senadeera, G.K.R.: Layered co-sensitization for enhancement of conversion efficiency of natural dye sensitized solar cells. J. Alloys. Compd. **581**, 186–191 (2013)
25. Ooyama, Y., Harima, Y.: Photophysical and electrochemical properties, and molecular structures of organic dyes for dye-sensitized solar cells. ChemPhysChem **13**(18), 4032–4080 (2012)
26. Chandra, N., Nath, D., Joon, H., Choi, W., Lee, J.: Electrochimica Acta Electrochemical approach to enhance the open-circuit voltage (V oc) of dye-sensitized solar cells (DSSCs). Electrochim. Acta **109**, 39–45 (2013)
27. Boschloo, G., Hagfeldt, A.: Characteristics of the iodide/triiodide redox mediator in dye-sensitized. Solar. Cells. **42**(11), 1819–1826 (2009)
28. Wang, P., Lovins, A.B., Zhang, G., Bai, Y., Li, R., Shi, D., Gra, M.: Employ a bisthienothiophene linker to construct an organic chromophore for efficient and stable dye-sensitized solar cells. Energy Environ. Sci. **2**(1), 1–5 (2009)
29. Gagliardi, S., Falconieri, M.: Experimental determination of the light-trapping-induced absorption enhancement factor in DSSC photoanodes. Beilstein. J. Nanotechnol. **6**(1), 886–892 (2015)
30. Tripathi, B., Yadav, P., Kumar, M.: Theoretical upper limit of short-circuit current density of TiO_2 nanorod based dye-sensitized solar cell. Results. Phys. **3**, 182–186 (2013)